Research
A SCIENCE PARTNER JOURNAL

RESEARCH ARTICLE

Amino Turbo Chirality and Its Asymmetric Control

Ting Xu[1], Yu Wang[1], Shengzhou Jin[1], Anis U. Rahman[2], Xianghua Yan[2], Qingkai Yuan[2], Hao Liu[2], Jia-Yin Wang[3], Wenxin Yan[4], Yinchun Jiao[4], Ruibin Liang[2*], and Guigen Li[1,2*]

[1]School of Chemistry and Chemical Engineering, Nanjing University, Nanjing 210093, China. [2]Department of Chemistry and Biochemistry, Texas Tech University, Lubbock, TX 79409-1061, USA. [3]School of Pharmacy, Continuous Flow Engineering Laboratory of National Petroleum and Chemical Industry, Changzhou University, Changzhou, Jiangsu 213164, China. [4]School of Chemistry and Chemical Engineering, Key Laboratory of Theoretical Organic Chemistry and Functional Molecular, Ministry of Education, Hunan University of Science and Technology, Xiangtan, Hunan 411201, China.

*Address correspondence to: rliang@ttu.edu (R.L.); guigen.li@ttu.edu, guigenli@nju.edu.cn (G.L.)

Citation: Xu T, Wang Y, Jin S, Rahman AU, Yan X, Yuan Q, Liu H, Wang JY, Yan W, Jiao Y, et al. Amino Turbo Chirality and Its Asymmetric Control. *Research* 2024;7:Article 0474. https://doi.org/10.34133/research.0474

Submitted 13 July 2024
Revised 11 August 2024
Accepted 26 August 2024
Published 19 September 2024

A series of new targets containing 3 chiral elements of central, orientational, and turbo chirality have been designed and synthesized asymmetrically. The absolute configurations and conformations of these types of chirality were concurrently controlled by using chiral sulfonimine auxiliary and unambiguously determined by x-ray diffraction analysis. These targets include alpha unnatural amino acid derivatives, which may play an important role for drug design, discovery, and development. Three propellers of turbo framework are covalently connected to a chiral C(sp^3) center via C(sp^2)–C(sp^3) bonding along with a C–N axis, while one of them is orientated away from the same carbon chiral center. The turbo or propeller chirality is characterized by 2 types of molecular arrangements of propellers, clockwise (*PPP*) and counterclockwise (*MMM*), respectively. The turbo stereogenicity was found to depend on the center chirality of sulfonimine auxiliary instead of the chiral C(sp^3) center, i.e., (*S*)- and (*R*)-sulfinyl centers led to the asymmetric formation of *PPP*- and *MMM*-configurations, respectively. Computational studies were conducted on relative energies for rotational barriers of a turbo target along the C–N anchor and the transition pathway between 2 enantiomers meeting our experimental observations. This work is anticipated to have a broad impact on chemical, biomedical, and materials sciences in the future.

Introduction

The origin of life is mainly about the origin of chirality since it has been found in all living creatures on Earth in forms varying from microscopic living organisms (e.g., helical bacteria) to macroscopic objects (e.g., sea shells) [1–5]. Several types of homochirality widely exist in functional biomolecules, such as DNA/RNA, peptides/proteins, and carbohydrates governing life processes [6–8]. In modern medicine, drug action processes of pharmaceuticals often depend on chirality to impose their potency and selectivity to reduce dosages and unwanted side effects [8–10]. In materials science, CPL (circularly polarized light) research has becoming increasingly active and important since controlling chirality of corresponding compounds and materials plays a crucial role to achieve challenging optoelectronic properties [11–15]. In chemical synthesis, asymmetric synthesis and catalysis have been serving for these areas in the past half a century for generating new chiral small molecules and polymers in higher chemical yields and diastereo- and enantioselectivity [16–43].

The discovery and development of new chiral elements is an important aspect of research in organic chemistry and represents one of the most intriguing areas of asymmetric catalysis. So far, there have been following major types of chirality: central [16–18], axial [20–27], spiral [16,21], sandwich (metallic [35–36] and organo [42–47]), and turbo or propeller chirality in small molecules [48–50]; multilayer (rigid helical [13,51] and flexible folding [52,53]) and topological and inherent chirality [54,55] in macro and polymeric molecules. It is worth noting that our recent work on a new chirality, orientational chirality, is uniquely characterized by C(sp^2)–C(sp^3) or C(sp)–C(sp^3) axis-anchored chiral centers and remotely anchored blockers [56–58] (Fig. 1). X-ray structural analysis has proven that individual orientational isomers can be stabilized by through-space functional groups; this enables one *R*- or *S*-chiral center to give 3 orientatiomers by rotating along the C(sp^2)–C(sp^3) or C(sp)–C(sp^3) axis. The orientational model was fundamentally different from the well-known Felkin–Ahn-type or Cram-type models in which chiral C(sp^3) center and blocking C(sp^2) carbons are adjacently anchored, leading to 6 energy barriers during rotating operation. However, in orientational chirality, there are 3 energy barriers for either (*R*)- or (*S*)-stereogenicity (Fig. 1). This is due to the fact that

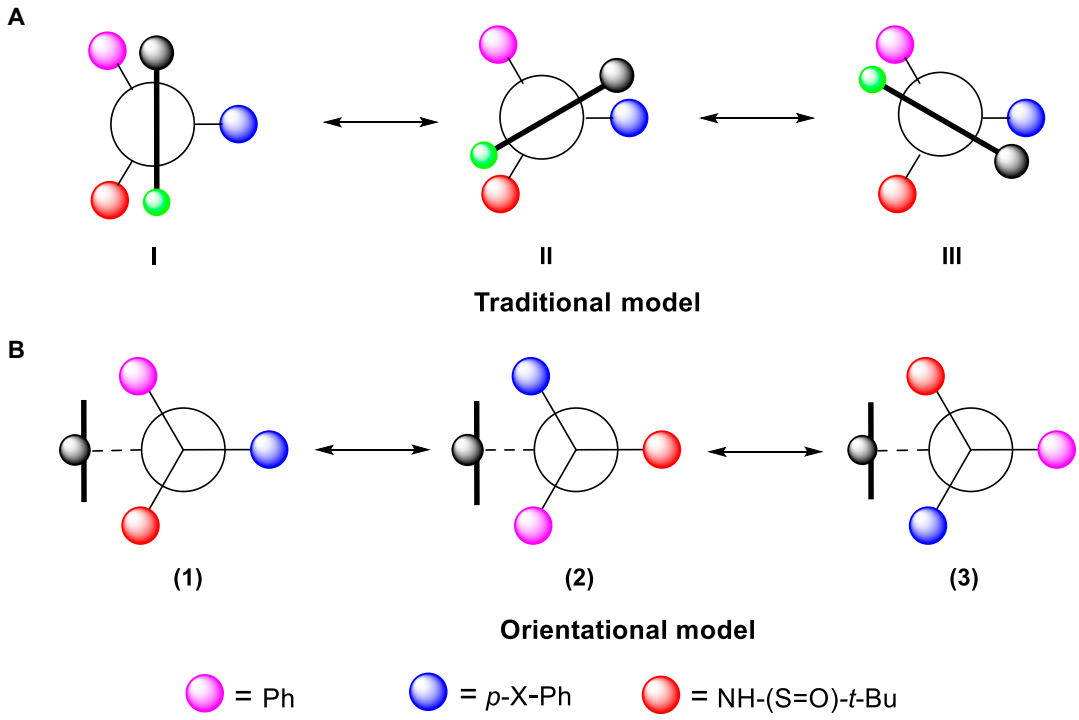

Fig. 1. Felkin–Ahn (A) and orientational (B) chirality models.

there exists a the steric dialog between the chiral C(sp^3) center and its remotely anchored blocker.

During our ongoing effort on seeking new orientational molecules, we now found that the chiral or achiral C(sp^3) center can be surrounded by 3 planar moieties with 2 types of arrangements of clockwise and counterclockwise fashions, which belong turbo or propeller chirality (Fig. 2). This turbo chirality originated from a chiral sulfur center of sulfinyl amide, which controls 3 chiral elements at the same time: C(sp^3) central, orientational, and turbo chirality. Surprisingly, the turbo chirality was solely controlled by the chiral sulfur center without being affected by the chiral C(sp^3) center as proven by generating achiral C(sp^3) centers as shown by x-ray diffraction analysis (Fig. 3). It is worth mentioning that over 75% of drugs contain amino functionality and more and more drugs have chiral center. The turbo amino chirality would provide more opportunities for chiral drug design and development in the future. Herein in this report, we would like to present our preliminary results on this new molecular framework.

Results

The present work was initiated by our design and synthesis of chiral unnatural amino acids with orientational chirality for peptide and protein research [8,56–58]. Introducing carboxylic ester and amine functionalities to the C(sp^3) center would serve for this purpose. It is well known that in traditional amino acids, one (*R*)- or (*S*)-chiral carbon center only corresponds to one chiral amino acid isomer. However, the number of chiral amino acid isomers would be increased 3 times more if their orientational chirality is taken into account. The use of naphthyl ring as the structural template for the synthesis of orientational amino acid derivatives would serve for this purpose, which has been proven to be successful in our previous similar design. Obviously, the substitution of hydrogen atom on position 1 of

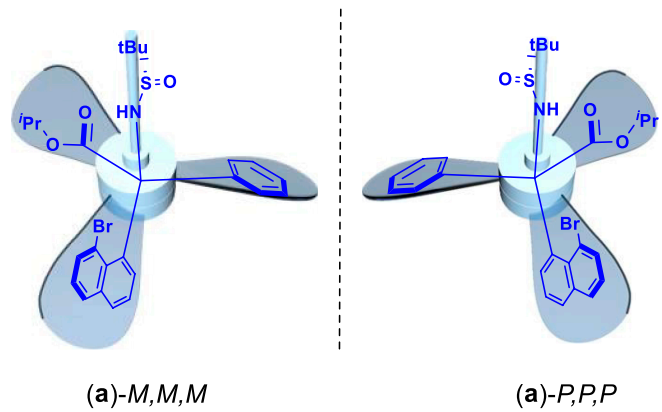

Fig. 2. Turbo chiral targets via 2 rotational operations along the C–N axis [orientational chirality was also shown by Ph being pushed away from Br].

naphthyl ring with larger moieties, such as Me, MeO, and Br, is anticipated to impose steric effects, so 1 of the 3 groups of the chiral C(sp^3) center on naphthyl position 8 is pushed away from them. Bromine substitution is the first case we investigated since we believe that heavy atom effect would benefit forming crystals for resulting products. Fortunately, based on this analysis, high-quality crystals of 2 individual enantiomers of the corresponding products were obtained smoothly. Their x-ray diffraction analysis proved that the phenyl ring of chiral carbon center is pushed away from the Br blocker, while isopropyl ester and *N*-sulfinyl groups are placed on each side of naphthyl ring in each case [(a)-*M,M,M* and (a)-*P,P,P* in Fig. 2].

The structural characteristics and nomenclature of the present turbo or propeller chirality directly benefits from known chiral targets, especially those of chiroptical switch molecules invented by the Nobel laureate Ben L. Feringa [59]. In those cases, alkenes are used as a centrally overcrowded anchor and

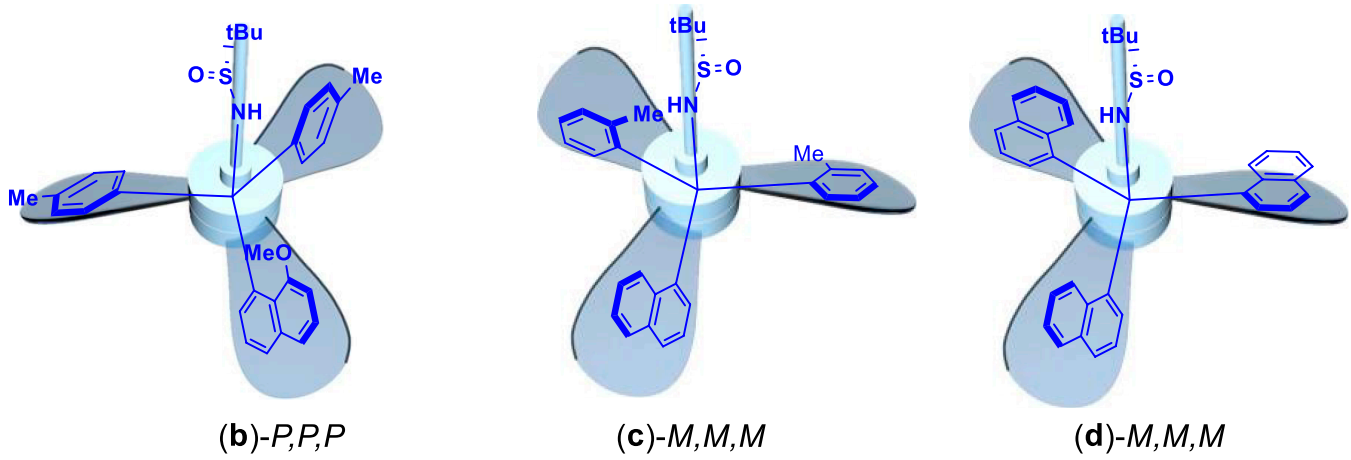

Fig. 3. Turbo chiral molecules centered by achiral carbon.

connected by 2 propeller blades with 2 chiral centers (Fig. 4). However, in our new targets, a chiral carbon center serves as a central anchor connected by 3 propellers and an amino moiety with chiral sulfur. As shown in Fig. 3, the chiral carbon center is unnecessary to achieve turbo chiral arrangement since 2 or 3 identical aromatic rings can be attached onto it, still showing 3 propellers of clockwise or anticlockwise arrangements depending on the chirality of amino protection auxiliary.

Asymmetric synthesis of turbo products is represented by assembling isopropyl 2-(8-bromonaphthalen-1-yl)-2-(((*S*)-*tert*-butylsulfinyl)amino)-2-phenylacetate [(**a**)-*M,M,M* in Figs. 2 and 5]. It was started by preparing the first building block **A2** through dehydration of (*R*)-2-methylpropane-2-sulfinamide with ethyl 2-oxo-2-phenylacetate **A1** by the use of $Ti(OEt)_4$ in dried tetrahydrofuran (THF) at 75 °C and then to room temperature to give isopropyl (*R,Z*)-2-((*tert*-butylsulfinyl)imino)-2-phenylacetate **A2** in a chemical yield of 85% (equation A, Fig. 5) [60,61]. 1,8-Dibromonaphthalene was pre-converted to its mono-lithium reagent by treating with butyllithium at −78 °C, which then proceeded electrophilic addition in situ to give isopropyl (*R,Z*)-2-((tert-butyl sulfinyl)imino)-2-phenylacetate **A2** at the same temperature for 2 h. Chromatographic purification afforded the final a single isomeric product of isopropyl 2-(8-bromonaphthalen-1-yl)-2-(((*R*)-*tert*-butyl sulfinyl) amino)-2-phenylacetate (a)-*P,P,P* in 70% yield (equation B, Fig. 5). The absolute configuration of this isomeric product has been unambiguously proven by its x-ray diffraction analysis as shown in Fig. 5.

The similar asymmetric assembly of the opposite enantiomer of(**a**)-*P,P,P*,isopropyl 2-(8-bromonaphthalen-1-yl)-2-(((*S*)-*tert*-butylsulfinyl)amino)-2-phenylacetate [(**a**)-*M,M,M*] was performed by following the above procedure to give a chemical yield of 77% for the key step that is nearly identical to that of the former (Fig. 6). Its absolute configuration was also determined by x-ray diffraction analysis as shown in Fig. 6. Two x-ray structures clearly indicate turbo arrangements surrounding the chiral carbon center, showing that the (*S*)-carbon, (*R*)-*tert*-butylsulfinyl group corresponds to clockwise and (*R*)-carbon, (*S*)-*tert*-butylsulfinyl group to *anti*-clockwise (Figs. 5 and 6).

Along with the generation of isomeric product (**a**)-*P,P,P*, we expend this approach to a series of other turbo isomeric products by retaining 8-bromonaphthalen-1-yl substructure and

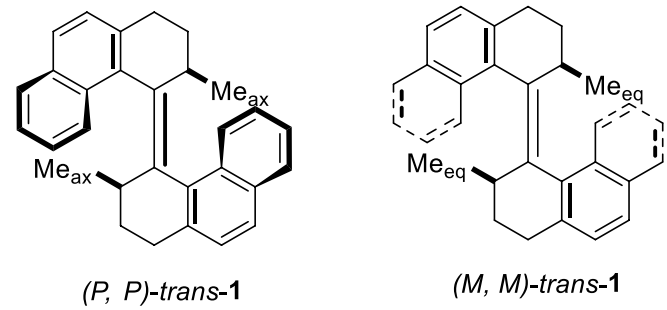

Fig. 4. Optical switching molecules centered by alkene.

changing Ph ring to other aromatic counterpart at first (Fig. 6). Symmetrically substituted 4-methyl and isopropyl phenyl substrates afforded turbo isomeric products, (**e**)-*P,P,P* and (**f**)-*P,P,P*, in chemical yields of 63% and 58%, respectively. The use of stronger electron-donation groups, MeO-[(**g**)-*P,P,P*] and nPro-[(**h**)-*P,P,P*] chemical yields of 80% and 55%, were obtained with a much higher yield for the former case but an almost identical yield for the latter. Three para-halogenated aryl (4-Br-, 4-Cl, and 4-F) and one ortho- and meta-F-Ph all resulted in turbo chiral products in chemical yields ranging from 56% to 81% [(**i**)-*P,P,P* to (**m**)-*P,P,P*; Fig. 6]. One strong electron-withdrawing group, 4-CF_3-Ph-attached aryl substrate, also worked well to give 67% yield ((**n**)-*P,P,P*). Second, the substrate change was made on the remaining 8-bromonaphthalen-1-yl substructure by replacing bromine with 3 other groups, Me-, MeO-, and Ac. Chemical yields of 71%, 85%, and 65% were achieved, respectively. The last substrate modification was made by introducing 2 MeO groups onto positions 2 and 7 of 8-bromonaphthalen-1-yl substructure. The expected turbo chiral product, isopropyl 2-(8-bromo-2,7-dimethoxynaphthalen-1-yl)-2-(((R)-*tert*-butylsulfinyl)amino)-2-phenylacetate (**r**)-*P,P,P*, was generated in 66% yield. Third, the substrate change was made by changing both iso-propyl ester to heterocycles of furan and thiophen and 8-bromonaphthalen-1-yl to 8-methoxylnaphthalen-1-yl counterpart. Individual enantiomers of (*R*)-*N*-(furan-3-yl(8-methoxynaphthalen-1-yl)(phenyl)methyl)-2-methylpropane-2-sulfinamide [(**s**)-*P,P,P*; Fig. 7] and (*R*)-*N*-((8-methoxynaphthalen-1-yl)(phenyl)(thiophen-2-yl)methyl)-2-methylpropane-2-sulfinamide [(**t**)-*P,P,P*; Fig. 7] were obtained in yields of 48% and 73%, respectively. More

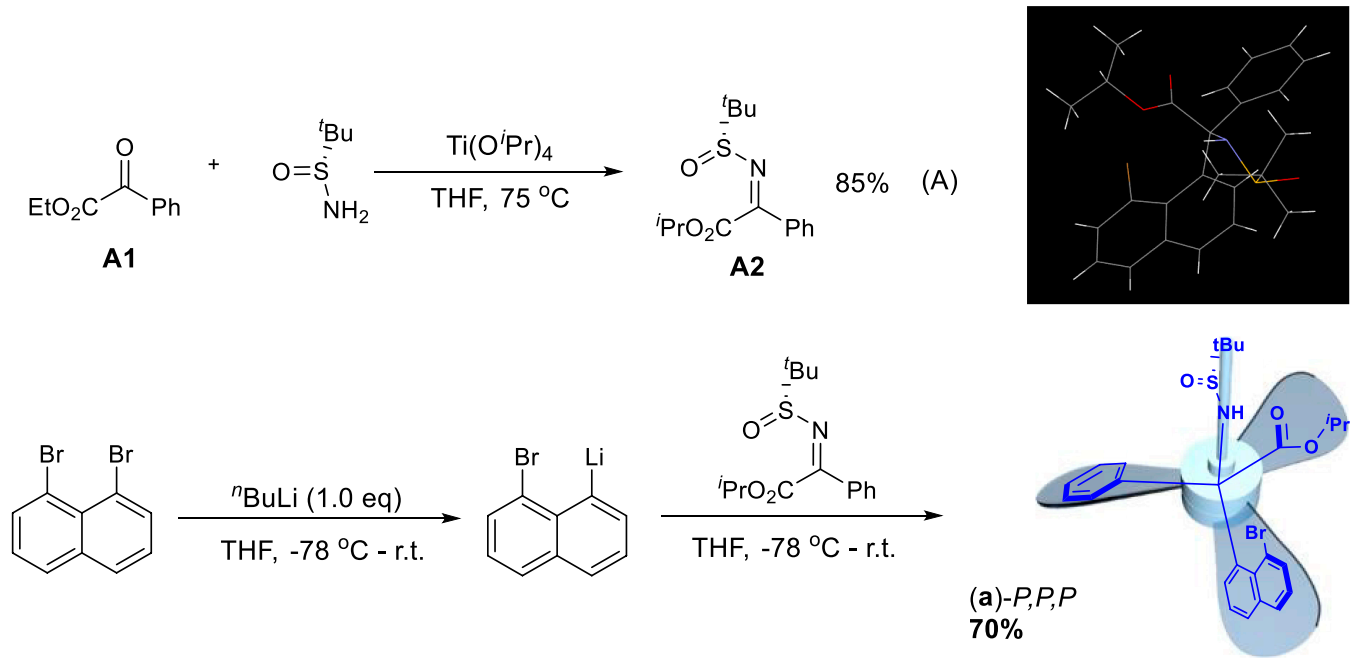

Fig 5. Asymmetric synthesis of turbo chiral (**a**)-*P,P,P* and its x-ray structure.

importantly, x-ray diffraction analysis revealed that both these turbo products display obvious clockwise absolute configurations, and both propeller blades of furan and thiophen rings are directed down-side away from sulfinyl group on chiral carbon center (Fig. 7).

To investigate whether chiral sulfur or carbon center control the turbo chirality predominantly, we utilized 2 and/or 3 identical aromatic groups to be anchored onto the central sp^3-carbon by using (*R*)-*N*-(di-tolylmethylene)-2-methylpropane-2-sulfinamide and (*S*)-*N*-(di(naphthalen-1-yl)methylene)-2-methylpropane-2-sulfinamide as electrophilic acceptors. These receptors that reacted with corresponding ArLi to give (*R*)-*N*-(di-*p*-tolylmethylene)-2-methylpropane-2-sulfinamide, (*S*)-N-(di-o-tolylmethylene)-2-methylpropane-2-sulfinamide, and(*S*)-N-(di(naphthalen-1-yl)methylene)-2-methylpropane-2-sulfinamide were synthesized in chemical yields of 47% [(**b**)-*P,P,P*], 60% [(**c**)-*M,M,M*], and 55% [(**d**)-*M,M,M*], respectively. To our pleasure, we were able to get good-quality crystals of these 3 turbo chiral products for x-ray structural analysis. Their x-ray structures confirmed that absolute turbo chirality depends on configuration of sulfur of sulfinamide instead of their sp^3 carbon centers. This means that (*R*)-*N*-propane-2-sulfinyl auxiliary leads to the formation of *P,P,P*-turbo chirality and (*S*)-*N*-propane-2-sulfinyl auxiliary results in the opposite *M,M,M*-turbo chirality. This conclusion can also be proven by the other 4 x-ray structures of 2 pairs of enantiomers controlling 2 opposite chiral auxiliaries as shown in Figs. 5 to 7.

We further employed quantum mechanics (QM) calculations at the density functional theory (DFT) level of theory to characterize the potential energies of stationary points (minima and transition states) along the minimum energy pathway (MEP) connecting (**d**)-*M,M,M* and (**d**)-*P,P,P* [62–72] (Fig. 8). These 2 enantiomers are referred to as Enantiomers 1 and 2 below, respectively. The results are summarized in Fig. 9. The computational results support the experimental findings that the center chirality of the sulfonimine auxiliary thermodynamically controls the turbo chirality of the 3 naphthalene rings. In particular, comparing Intermediate 1 and Enantiomer 1, which share the same center chirality of the sulfonimine auxiliary but differ in the turbo chirality of the 3 naphthalene rings, Intermediate 1 is 2.5 kcal/mol higher in energy due to changing the turbo chirality of the 3 rings. In other words, the lower energy of Enantiomer 1 perhaps arises from the more favorable van der Waals interaction between the sulfonimine auxiliary and the 3 hydrophobic naphthalene rings oriented in this chiral configuration. Thus, at equilibrium, the chirality of the sulfonimine auxiliary results in a higher population of the *MMM* turbo chiral configuration in Enantiomer 1 than the *PPP* configuration observed in Intermediate 1.

The transition between the 2 chiral configurations of 3 naphthalene rings is also kinetically slow. The TS separating Enantiomer 1 and Intermediate 1 has a high energy of 20.9 kcal/mol, implying a slow rate for changing the turbo chirality of the 3 rings, contributing to the kinetic stability of Enantiomer 1. The inversion of the central chirality of the sulfonimine auxiliary converts Intermediate 1 to Enantiomer 2. Enantiomer 2 is the mirror image of Enantiomer 1 and thus has the same energy as the latter. Starting from Intermediate 1, the inversion of the sulfonimine auxiliary's chirality needs to overcome a high kinetic barrier of 55.7 kcal/mol, leading to a significant overall kinetic barrier of 58.2 kcal/mol separating Enantiomers 1 and 2.

The extended computational work is currently being extended to other atom-centered turbo molecular frameworks in our laboratories. It is worth mentioning that although tri- or tetra-aromatic rings surrounding P- and C-centered compounds have been widely reported in literature [21–22,42,73–88], their turbo chirality patterns have not been paid attention for a while until recently when several groups were involved in this research (Fig. 10 and Supplementary Materials) [48–50,83–86]. In addition, we also found that turbo chirality exists in diaryl ethers with 2 propeller blades [88–91] and in multiple aryl

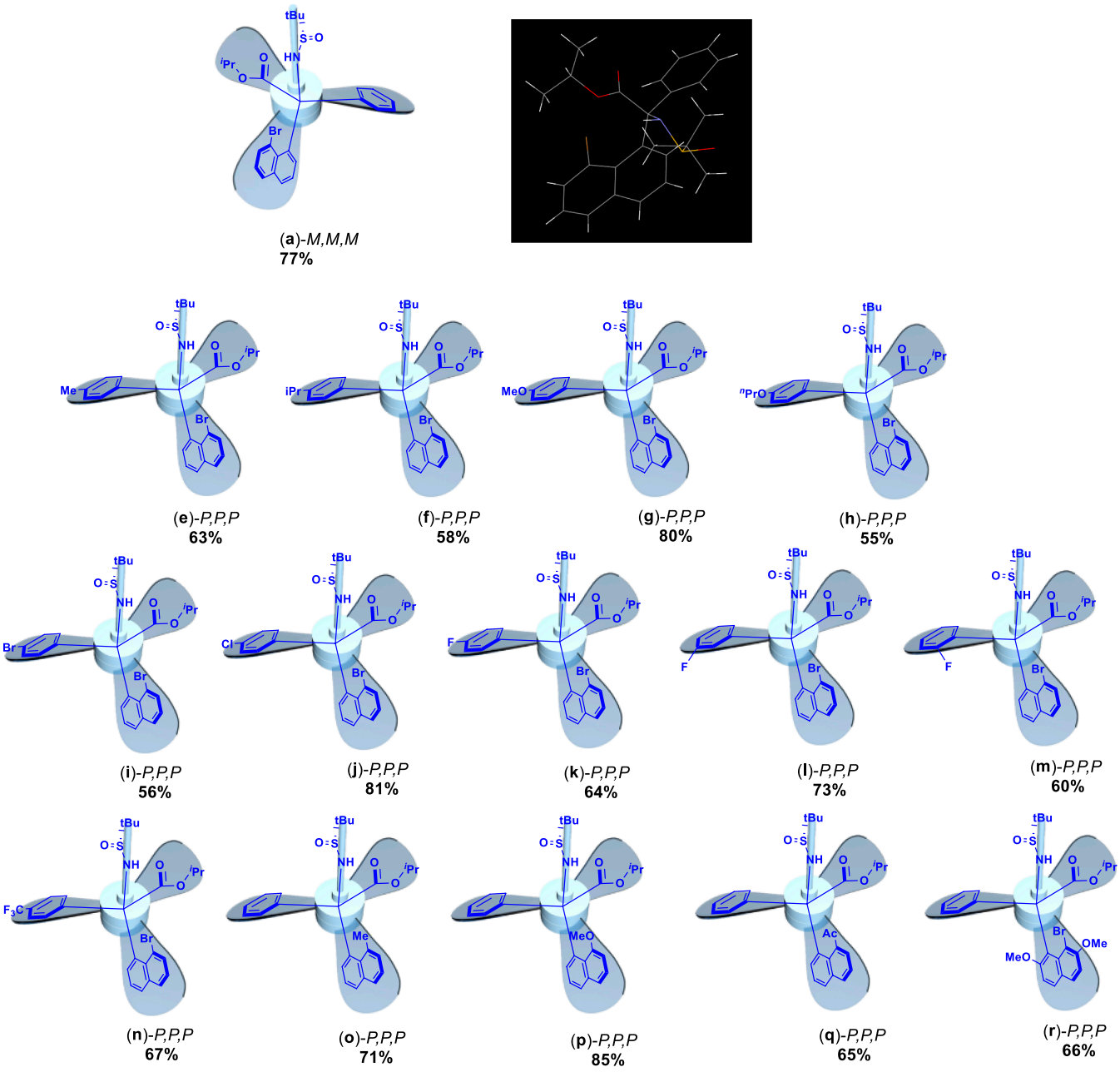

Fig. 6. Scope of asymmetric synthesis of turbo chiral compounds.

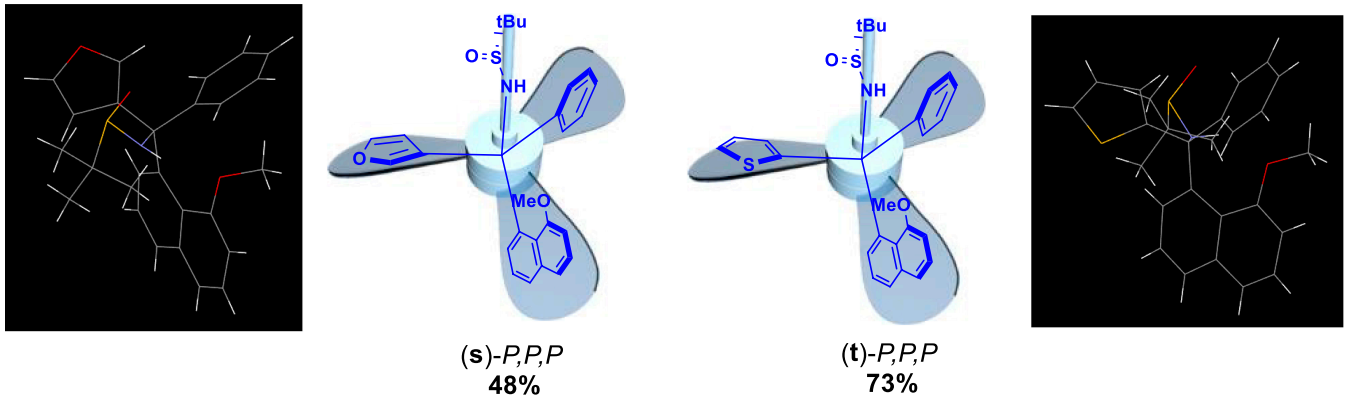

Fig. 7. Turbo chirality targets with heterocycles.

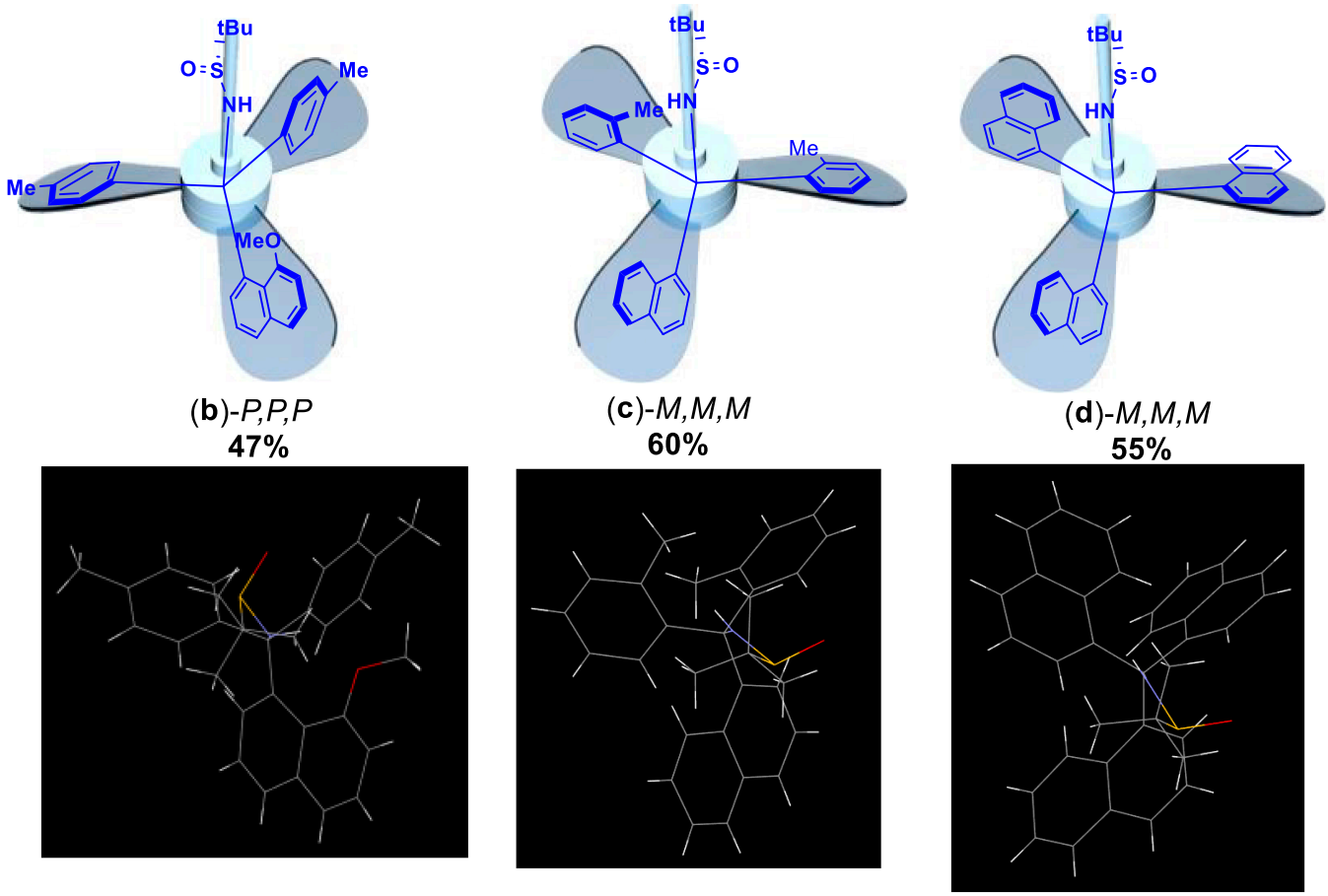

Fig. 8. Turbo chirality targets with achiral C(sp^3)-center.

ring-anchored structures with tri or tetra propeller blades ([87,92,93] and Supplementary Materials).

Discussion

We have designed and synthesized new chiral targets containing central, orientational, and turbo chirality surrounding a C–N axis. The chirality is efficiently controlled by sulfonimine auxiliary via asymmetric nucleophilic carbonyl addition reaction. The resulting configurations and conformations have been unambiguously confirmed by x-ray diffraction analysis. The turbo atropisomers are characterized by 2 types of molecular clockwise and counterclockwise arrangements of structural blades. The absolute *PPP*- and *MMM*-stereogenicity was proven to depend on the center chirality of sulfonimine auxiliary, i.e., (*S*)- and (*R*)-sulfinyl centers led to the asymmetric formation of complete *PPP*- and *MMM*-configurations, respectively, regardless of the center chirality of C(sp^3) joint. This was confirmed by attaching 2 or 3 identical aromatic blades onto the C(sp^3) joint of the C–N axis. Computational studies were performed to characterize the energy of the intermediate state and the barriers along the MEP between 2 enantiomers of (**d**). The computational results support our experimental finding that the turbo chirality of the compound is thermodynamically controlled by the center chirality of the sulfonimine auxiliary. Meanwhile, the chirality inversion of the sulfonimine auxiliary is the rate-limiting step for the transition between the *PPP*- and *MMM*-configurations. The high barriers along the reaction pathway prevent facile transition between them, allowing for the separation of distinct kinetically stable enantiomers in the experiment. The present turbo chirality work would be anticipated by enhancing a new stereochemistry topic and to have a broad impact on chemical, biomedical, and material sciences in the future.

Materials and Methods

Unless otherwise stated, all reactions were magnetically stirred and conducted in oven-dried glassware in anhydrous solvents under Ar, applying standard Schlenk techniques. Solvents and liquid reagents, as well as solutions of solid or liquid reagents were added via syringes, stainless steel, or polyethylene cannulas through rubber septa or through a weak Ar counterflow. Solvents were removed under reduced pressure at 40 to 65 °C using a rotavapor. All given yields are isolated yields of chromatographic and NMR spectroscopic materials. All commercially available chemicals were used as received without further purification.

^{1}H and ^{13}C nuclear magnetic resonance (NMR) spectra were recorded in $CDCl_3$ on 400-MHz instruments with trimethylsilyl (TMS) as internal standard. For referencing of the ^{1}H NMR spectra, the residual solvent signal ($\delta = 7.26$ ppm for $CDCl_3$) was used. In the case of the ^{13}C NMR spectra, the signal of solvent ($\delta = 77.0$ ppm for $CDCl_3$) was used. Chemical shifts

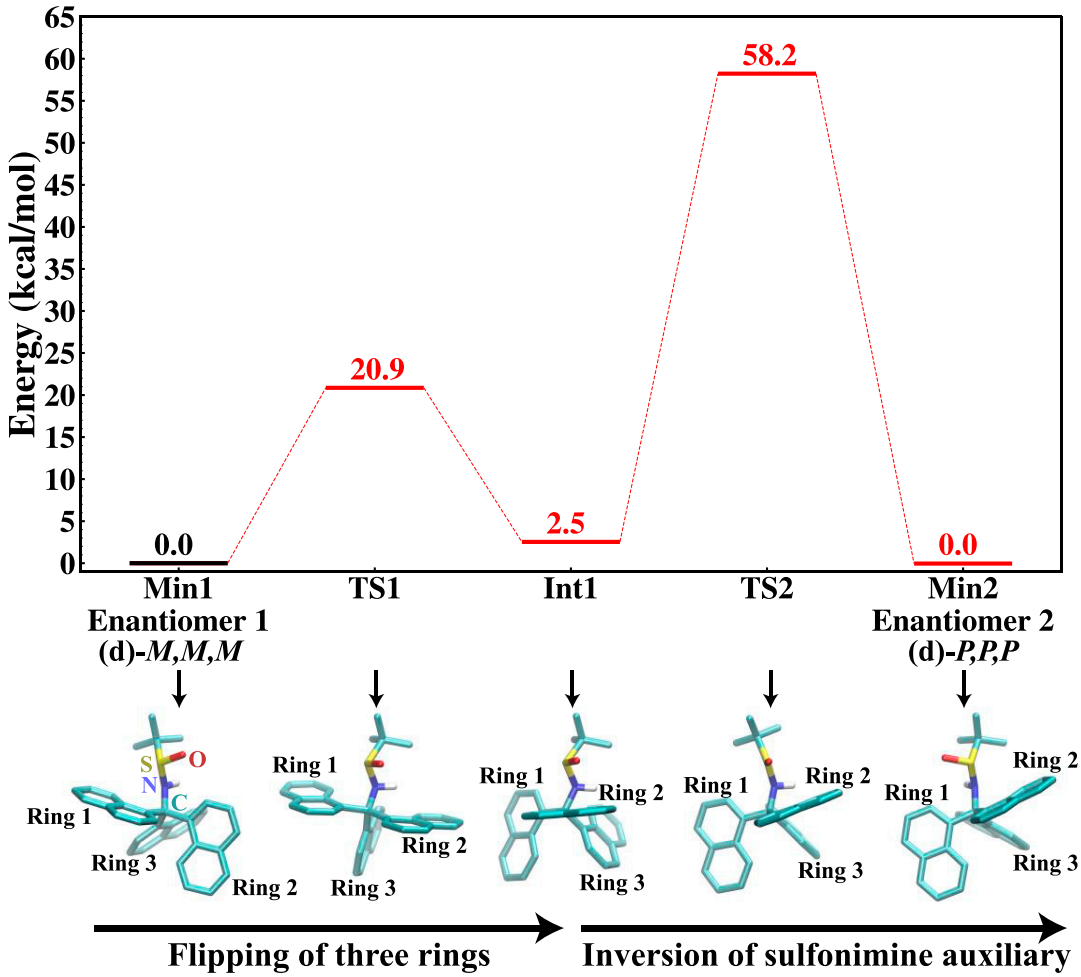

Fig. 9. Energy diagram for the reaction pathway from Enantiomer 1 to Enantiomer 2, which are mirror images of each other. The first stage of the pathway is the simultaneous flipping of the 3 naphthalene rings, overcoming transition state 1 (TS1) and resulting in an intermediate (Int1). The second stage is the inversion of the sulfonimine auxiliary, overcoming transition state 2 (TS2) and resulting in an Enantiomer 2. Structures of the stationary points along the pathway (minima and transition states) are illustrated below the energy diagram. Key functional groups are labeled, including the central atoms (C, N, S, O atoms) in the axis of the ring-flipping motion. All energies are evaluated using the B3LYP-D3/def2-TZVP method at the stationary points optimized with the B3LYP-D3/def2-SVP method. The zero point energy (ZPE) corrections have been included at the B3LYP-D3/def2-SVP level of theory at the optimized stationary points. The higher energy of Int1 than Enantiomer 1 and 2 indicates that the sulfonimine auxiliary thermodynamically controls the turbo chirality of the 3 naphthalene rings. Also, the considerable kinetic barriers for both stages of the transition contribute to the kinetic stability of the 2 enantiomers.

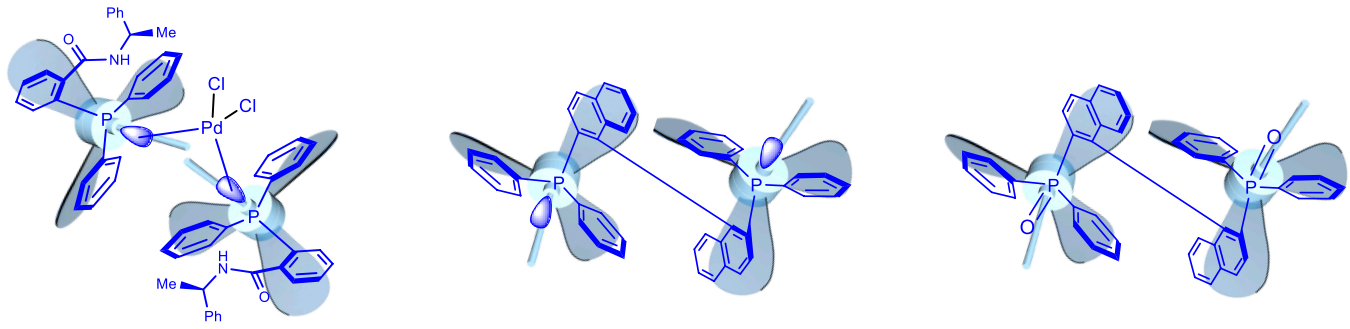

Fig. 10. Turbo chirality with 2 units of triple propeller blades of chiral ligands and complex.

(δ) were reported in ppm with respect to TMS. Data are represented as follows: chemical shift, multiplicity (s = singlet, d = doublet, t = triplet, m = multiplet), coupling constant (*J*, Hz), and integration. Optical rotations were measured with a Rudolph Research Analytical APIV/2 W Polarimeter at the indicated temperature with a sodium lamp. Measurements were performed in a 2-ml vessel with the concentration unit of g/100 ml in the corresponding solvents.

The details of computational methods are included in the Supplementary Materials, which include the selection of initial

geometries, the QM level of theory, and the optimization of the stationary points along the reaction pathway.

Acknowledgments

Funding: We would like to acknowledge the financial support from Robert A. Welch Foundation [D-1361-20210327, USA (G.L.), D-2108-20220331 (R.L.)] and the National Natural Science Foundation of China (nos. 22071102 and 91956110).
Author contributions: G.L. and R.L. directed the research and wrote the paper. T.X., Y.W., S.J., A.U.R., X.Y., Q.Y., H.L., and J.-Y.W. performed and repeated all synthetic experiments and data analysis. W.Y., Y.J., and R.L. conducted computations and wrote relevant parts.
Competing interests: The authors declare that they have no competing interests.

Data Availability

All data are available in the manuscript or Supplementary Materials.

Supplementary Materials

Supplementary Text
Figs. S1 to S48
Table S1
Computational Methods

References

1. Taniguchi K, Maeda R, Ando T, Okumura T, Nakazawa N, Hatori R, Nakamura M, Hozumi S, Fujiwara H, Matsuno K. Chirality in planar cell shape contributes to left-right asymmetric epithelial morphogenesis. *Science*. 2011;333(6040):339–341.
2. Wang AH-J, Fujii S, van Boom JH, Rich A. Right-handed and left-handed double-helical DNA: Structural studies. *Cold Spring Harb Symp Quant Biol*. 1983;47:33–44.
3. Krautwald S, Sarlah D, Schafroth MA, Carreira EM. Enantio- and diastereodivergent dual catalysis: A-allylation of branched aldehydes. *Science*. 2013;340(6136):1065–1068.
4. Zhang J, Kürti L. Multi-layer 3D chirality: Its enantioselective synthesis and aggregation-induced emission. *Natl Sci Rev*. 2021;8(1):nwaa205.
5. Bryliakov KP. Chemical mechanisms of prebiotic chirality amplification. *Research*. 2020;2020:5689246.
6. Wagner I, Musso H. New naturally occurring amino acids. *Angew Chem Int Ed Engl*. 1983;22(11):816–828.
7. Dunitz JD. Pauling's left-handed α-helix. *Angew Chem Int Ed Engl*. 2001;40(22):4167–4173.
8. Hruby VJ, Li G, Haskell-Luevano C, Shenderovich M. Design of peptides, proteins, and peptidomimetics in chi space. *Biopolymers*. 1997;43(3):219–266.
9. Smith DA, Jones RM. The sulfonamide group as a structural alert: A distorted story? *Curr Opin Drug Discov Devel*. 2008;11(1):72–79.
10. Tang X, Fang M, Cheng R, Niu J, Huang X, Xu K, Wang G, Sun Y, Liao Z, Zhang Z, et al. Transferrin is up-regulated by microbes and acts as a negative regulator of immunity to induce intestinal immunotolerance. *Research*. 2024;7:0301.
11. Hu M, Feng H-T, Yuan Y-X, Zheng Y-S, Tang BZ. Chiral AIEgens–Chiral recognition, CPL materials and other chiral applications. *Coord Chem Rev*. 2020;416:213329.
12. Bao J, Liu N, Tian H, Wang Q, Cui T, Jiang W, Zhang S, Cao T. Chirality enhancement using Fabry–Pérot-like cavity. *Research*. 2020;2020:7873581.
13. Shen Y, Chen C-F. Helicenes: Synthesis and applications. *Chem Rev*. 2012;112(3):1463–1535.
14. Oki O, Kulkarni C, Yamagishi H, Meskers SCJ, Lin Z-H, Huang J-S, Meijer EW, Yamamoto Y. Robust angular anisotropy of circularly polarized luminescence from a single twisted-bipolar polymeric microsphere. *J Am Chem Soc*. 2021;143(23):8772–8779.
15. Liu T-T, Yan Z-P, Hu J-J, Yuan L, Luo X-F, Tu Z-L, Zheng Y-X. Chiral thermally activated delayed fluorescence emitters-based efficient circularly polarized organic light-emitting diodes featuring low efficiency roll-off. *ACS Appl Mater Interfaces*. 2021;13(47):56413–56419.
16. Zhou Q-L, *Privileged chiral ligands and catalysts*. Weinheim (Germany): Wiley-VCH Verlag; 2011.
17. Zhao P, Li Z, He J, Liu X, Feng X. Asymmetric catalytic 1,3-dipolar cycloaddition of α-diazoesters for synthesis of 1-pyrazoline-based spirochromanones and beyond. *Sci China Chem*. 2021;64:1355–1360.
18. Wright TB, Evans PA. Catalytic enantioselective alkylation of prochiral enolates. *Chem Rev*. 2021;121(15):9196–9242.
19. Wang G, Zhang M, Guan Y, Zhang Y, Hong X, Wei C, Zheng P, Wei D, Fu Z, Chi YR, et al. Desymmetrization of cyclic 1,3-diketones under *N* -heterocyclic carbene organocatalysis: Access to organofluorines with multiple stereogenic centers. *Research*. 2021;2021:9867915.
20. Liu D, Li B, Chen J, Gridnev ID, Yan D, Zhang W. Ni-catalyzed asymmetric hydrogenation of N-aryl imino esters for the efficient synthesis of chiral α-aryl glycines. *Nat Commun*. 2020;11(1):5935.
21. Cao Z-Y, Wang X, Tan C, Zhao X-L, Zhou J, Ding K. Highly stereoselective olefin cyclopropanation of diazooxindoles catalyzed by a C_2-symmetric spiroketal bisphosphine/Au(I) complex. *J Am Chem Soc*. 2013;135(22):8197–8200.
22. Ge Y, Qin C, Bai L, Hao J, Liu J, Luan X. A dearomatization/debromination strategy for the [4+1] spiroannulation of bromophenols with α,β-unsaturated imines. *Angew Chem Int Ed*. 2020;59(43):18985–18989.
23. Wang Q, Zhang W-W, Zheng C, Gu Q, You S-L. Enantioselective synthesis of azoniahelicenes by Rh-catalyzed C–H annulation with alkynes. *J Am Chem Soc*. 2021;143(1):114–120.
24. Reimann S, Adachi S, Subramanian H, Sibi MP. Enantioselective enolate protonations: Evaluation of achiral templates with fluxional brønsted basic substituents in conjugate addition of malononitriles. *Tetrahedron*. 2024;152:133833.
25. Wang Y-B, Tan B. Construction of axially chiral compounds via asymmetric organocatalysis. *Acc Chem Res*. 2018;51:534–547.
26. Liao G, Yao Q-J, Zhang Z-Z, Wu Y-J, Huang D-Y, Shi B-F. Scalable, stereocontrolled formal syntheses of (+)-isoschizandrin and (+)-steganone: Development and applications of palladium(II)-catalyzed atroposelective C−H alkynylation. *Angew Chem Int Ed*. 2018;57(14):3661–3665.
27. Liu Y, Li W, Zhang J. Chiral ligands designed in China. *Natl Sci Rev*. 2017;4(3):326–358.

28. Huang S, Wen H, Tian Y, Wang P, Qin W, Yan H. Organocatalytic enantioselective construction of chiral azepine skeleton bearing multiple-stereogenic elements. *Angew Chem Int Ed*. 2021;60(39):21486–21493.
29. Cui X, Xu X, Lu H, Zhu S, Wojtas L, Zhang XP. Enantioselective cyclopropenation of alkynes with acceptor/acceptor-substituted diazo reagents via Co(II)-based metalloradical catalysis. *J Am Chem Soc*. 2011;133(10):3304–3307.
30. Ma C, Sheng F-T, Wang H-Q, Deng S, Zhang Y-C, Jiao Y, Tan W, Shi F. Atroposelective access to oxindole-based axially chiral styrenes via the strategy of catalytic kinetic resolution. *J Am Chem Soc*. 2020;142(37):15686–15696.
31. Wu R, Lu J, Cao T, Ma J, Chen K, Zhu S. Enantioselective Rh(II)-catalyzed desymmetric cycloisomerization of diynes: Constructing furan-fused dihydropiperidines with an alkyne-substituted aza-quaternary stereocenter. *J Am Chem Soc*. 2021;143(36):14916–14925.
32. Chai Z, Zhao G. Efficient organocatalysts derived from simple chiral acyclic amino acids in asymmetric catalysis. *Cat Sci Technol*. 2012;2:29–41.
33. Luo S, Xu H, Li J, Zhang L, Cheng J-P. A simple primary–tertiary diamine–Brønsted acid catalyst for asymmetric direct aldol reactions of linear aliphatic ketones. *J Am Chem Soc*. 2007;129(11):3074–3075.
34. Chen J-R, Lu H-H, Li X-Y, Cheng L, Wan J, Xiao W-J. Readily tunable and bifunctional l-prolinamide derivatives: Design and application in the direct enantioselective aldol reactions. *Org Lett*. 2005;7(20):4543–4545.
35. Dai L-X, Tu T, You S-L, Deng W-P, Hou X-L. Asymmetric catalysis with chiral ferrocene ligands. *Acc Chem Res*. 2003;36(9):659–667.
36. Fu GC. Enantioselective nucleophilic catalysis with "planar-chiral" heterocycles. *Acc Chem Res*. 2000;33(6):412–420.
37. Zhou Y, Zhang X, Liang H, Cao Z, Zhao X, He Y, Wang S, Pang J, Zhou Z, Ke Z, et al. Enantioselective synthesis of axially chiral biaryl monophosphine oxides via direct asymmetric Suzuki coupling and DFT investigations of the enantioselectivity. *ACS Catal*. 2014;4(5):1390–1397.
38. Zhang R, Ge S, Sun J. Correction to "SPHENOL, A New Chiral Framework for Asymmetric Synthesis". *J Am Chem Soc*. 2021;143(42):12445–12449.
39. Chen X-Y, Gao Z-H, Ye S. Bifunctional N-heterocyclic carbenes derived from l-pyroglutamic acid and their applications in enantioselective organocatalysis. *Acc Chem Res*. 2020;53(3):690–702.
40. Rouh H, Tang Y, Xu T, Yuan Q, Zhang S, Wang J-Y, Jin S, Wang Y, Pan J, Wood HL, et al. Aggregation-induced synthesis (AIS): Asymmetric synthesis via chiral aggregates. *Research*. 2022;2022:9865108.
41. Tang Y, Wang Y, Yuan Q, Zhang S, Wang J-Y, Jin S, Xu T, Pan J, Surowiec K, Li G. Aggregation-induced catalysis: Asymmetric catalysis with chiral aggregates. *Research*. 2023;6:0163.
42. Wu G, Liu Y, Rouh H, Ma L, Tang Y, Zhang S, Zhou P, Wang J-Y, Jin S, Unruh D, et al. Asymmetric catalytic approach to multilayer 3D chirality. *Chemistry*. 2021;27(30):8013–8020.
43. Wu G, Liu Y, Yang Z, Katakam N, Rouh H, Ahmed S, Unruh D, Surowiec K, Li G. Multilayer *3D* chirality and its synthetic assembly. *Research*. 2019;2019:6717104.
44. Wu G, Liu Y, Yang Z, Jiang T, Katakam N, Rouh H, Ma L, Tang Y, Ahmed S, Rahman AU, et al. Enantioselective assembly of multi-layer *3D* chirality. *Natl Sci Rev*. 2020;7(3):588–599.
45. Liu Y, Wu G, Yang Z, Rouh H, Katakam N, Ahmed S, Unruh D, Cui Z, Lischka H, Li G. Multi-layer 3D chirality: New synthesis, AIE and computational studies. *Sci China Chem*. 2020;63:692–698.
46. Jin S, Wang J-Y, Tang Y, Rouh H, Zhang S, Xu T, Wang Y, Yuan Q, Chen D, Unruh D, et al. Central-to-folding chirality control: Asymmetric synthesis of multilayer 3D targets with electron-deficient bridges. *Front Chem*. 2022;10:860398.
47. Tang Y, Wu G, Jin S, Liu Y, Ma L, Zhang S, Rouh H, Ali AIM, Wang J-Y, Xu T, et al. From center-to-multilayer chirality: Asymmetric synthesis of multilayer targets with electron-rich bridges. *J Org Chem*. 2022;87(9):5976–5986.
48. Kong Y-J, Yan Z-P, Li S, Su H-F, Li K, Zheng Y-X, Zang S-Q. Photoresponsive propeller-like chiral AIE copper(I) clusters. *Angew Chem Int Ed Engl*. 2020;59(13):5336–5340.
49. Kemper M, Reese S, Engelage E, Merten C. Inducing propeller chirality in triaryl boranes with chiral amines. *Chemistry*. 2022;28(70):Article e202202812.
50. Kótai B, Laczkó G, Hamza A, Pápai I. Stereocontrol via propeller chirality in FLP-catalyzed asymmetric hydrogenation. *Chemistry*. 2024;30(21):Article e202400241.
51. Shirakawa S, Liu S, Kaneko S. Organocatalyzed asymmetric synthesis of axially, planar, and helical chiral compounds. *Chem Asian J*. 2016;11(3):330–341.
52. Wang J-Y, Tang Y, Wu G-Z, Zhang S, Rouh H, Jin S, Xu T, Wang Y, Unruh D, Surowiec K, et al. Asymmetric catalytic assembly of triple-columned and multilayered chiral folding polymers showing aggregation-induced emission (AIE). *Chemistry*. 2022;28(7):Article e202104102.
53. Tang Y, Jin S, Zhang S, Wu G-Z, Wang J-Y, Xu T, Wang Y, Unruh D, Surowiec K, Ma Y, et al. Multilayer 3D chiral folding polymers and their asymmetric catalytic assembly. *Research*. 2022;2022:9847949.
54. Zhang D-Y, Sang Y, Das TK, Guan Z, Zhong N, Duan C-G, Wang W, Fransson J, Naaman R, Yang H-B. Highly conductive topologically chiral molecular knots as efficient spin filters. *J Am Chem Soc*. 2023;145(49):26791–26798.
55. Tong S, Li J-T, Liang D-D, Zhang Y-E, Feng Q-Y, Zhang X, Zhu J, Wang M-X. Catalytic enantioselective synthesis and switchable chiroptical property of inherently chiral macrocycles. *J Am Chem Soc*. 2020;142(34):14432–14436.
56. Jin S, Wang Y, Tang Y, Wang J-Y, Xu T, Pan J, Zhang S, Yuan Q, Rahman AU, McDonald JD, et al. Orientational chirality, its asymmetric control, and computational study. *Research*. 2022;2022:0012.
57. Jin S, Xu T, Tang Y, Wang J-Y, Wang Y, Pan J, Zhang S, Yuan Q, Rahman AU, Aquino AJA, et al. A new chiral phenomenon of orientational chirality, its synthetic control and computational study. *Front Chem*. 2023;10:1110240.
58. Xu T, Wang J-Y, Wang Y, Jin S, Tang Y, Zhang S, Yuan Q, Liu H, Yan W, Jiao Y, et al. C(sp)-C(sp) lever-based targets of orientational chirality: Design and asymmetric synthesis. *Molecules*. 2024;29(10):2274.
59. Feringa BL. The art of building small: From molecular switches to motors (Nobel lecture). *Angew Chem Int Ed*. 2017;56(37):11060–11078.
60. Davis FA, Chen B-C. Asymmetric synthesis of amino acids using sulfinimines (thiooxime S-oxides). *Chem Soc Rev*. 1998;27(1):13–18.

61. Robak MT, Herbage MA, Ellman JA. Synthesis and applications of *tert*-butanesulfinamide. *Chem Rev*. 2010;110(6):3600–3740.
62. Qu C, Deng S, Cheng Q, Jiao Y, Tang Z, Liu W. Theoretical study on aggregation-induced emission of new multi-layer 3D chiral molecules. *Mol Simul*. 2022;48(12):1102–1111.
63. Becke AD. Density-functional exchange-energy approximation with correct asymptotic behavior. *Phys Rev A Gen Phys*. 1988;38(6):3098–3100.
64. Lee C, Yang W, Parr RG. Development of the Colle-Salvetti correlation-energy formula into a functional of the electron density. *Phys Rev B Condens Matter*. 1988;37(2):785–789.
65. Becke AD. Density-functional thermochemistry. III. The role of exact exchange. *J Chem Phys*. 1993;98:5648–5652.
66. Becke AD. A new mixing of Hartree–Fock and local density-functional theories. *J Chem Phys*. 1993;98(2):1372–1377.
67. Grimme S, Antony J, Ehrlich S, Krieg H. A consistent and accurate *ab initio* parametrization of density functional dispersion correction (DFT-D) for the 94 elements H-Pu. *J Chem Phys*. 2010;132(15):154104.
68. Weigend F, Ahlrichs R. Balanced basis sets of split valence, triple zeta valence and quadruple zeta valence quality for H to Rn: Design and assessment of accuracy. *Phys Chem Phys*. 2005;7(18):3297–3305.
69. Kästner J, Sherwood P. Superlinearly converging dimer method for transition state search. *J Chem Phys*. 2008;128(1):Article 014106.
70. Balasubramani SG, Chen GP, Coriani S, Diedenhofen M, Frank MS, Franzke YJ, Furche F, Grotjahn R, Harding ME, Hättig C, et al. TURBOMOLE: Modular program suite for *ab initio* quantum-chemical and condensed-matter simulations. *J Chem Phys*. 2020;152(18):184107.
71. Kästner J, Carr JM, Keal TW, Thiel W, Wander A, Sherwood P. DL-FIND: An open-source geometry optimizer for atomistic simulations. *J Phys Chem A*. 2009;113(43):11856–11865.
72. Metz S, Kästner J, Sokol AA, Keal TW, Sherwood P. ChemShell—A modular software package for QM/MM simulations. *Wiley Interdiscip. Rev. Comput. Mol. Sci.* 2014;4(2):101–110.
73. Tang W, Zhang X. New chiral phosphorus ligands for enantioselective hydrogenation. *Chem Rev*. 2003;103(8): 3029–3070.
74. Luo C, Yin Y, Jiang Z. Recent advances in asymmetric synthesis of P-chiral phosphine oxides. *Youji Huaxue*. 2023;43(6):1963.
75. Zhu R-Y, Liao K, Yu J-S, Zhou J. Recent advances in catalytic asymmetric synthesis of *P*-chiral phosphine oxides. *Huaxue Xuebao*. 2020;78(3):193.
76. Xue Q, Huo S, Wang T, Wang Z, Li J, Zhu M, Zuo W. Diastereoselective synthesis of P-chirogenic and atropisomeric 2,2′-bisphosphino-1,1′-binaphthyls enabled by internal phosphine oxide directing groups. *Angew Chem Int Ed Engl*. 2020;59(21):8153–8159.
77. Zhang Y, Zhang F, Chen L, Xu J, Liu X, Feng X. Asymmetric synthesis of *P*-stereogenic compounds via thulium (III)-catalyzed desymmetrization of dialkynylphosphine oxides. *ACS Catal*. 2019;9(6):4834–4840.
78. Wang X, Lu S-M, Li J, Liu Y, Li C. Conjugated microporous polymers with chiral BINAP ligand built-in as efficient catalysts for asymmetric hydrogenation. *Cat Sci Technol*. 2015;5:2585–2589.
79. Xu G, Senanayake CH, Tang W. P-chiral phosphorus ligands based on a 2,3-dihydrobenzo[*d*][1,3]oxaphosphole motif for asymmetric catalysis. *Acc Chem Res*. 2019;52(4):1101–1112.
80. Nie S-Z, Davison RT, Dong VM. Enantioselective coupling of dienes and phosphine oxides. *J Am Chem Soc*. 2018;140(48):16450–16454.
81. Li W, Zhang J. Sadphos as adaptive ligands in asymmetric palladium catalysis. *Acc Chem Res*. 2024;57(4):489–513.
82. Guo R, Liu Z, Zhao X. Efficient synthesis of P-chirogenic compounds enabled by chiral selenide-catalyzed enantioselective electrophilic aromatic halogenation. *CCS Chem*. 2021;3:2617–2628.
83. Jin S. Synthesis of multiple-layered folding chiral molecules and study on guided C-H activation to construct C-C/Si bond [thesis]. [Nanjing (China)]: Nanjing University; 2024.
84. Li G. New members of chirality family—Turbo and staircase chirality. U.S. Patent #63/642,932. May 6, 2024.
85. Li G. New turbo chiral targets with propeller blades centered by various atoms. U.S. Patent #63/678,537. August 2, 2024.
86. Liu J, Deng R, Liang X, Zhou M, Zheng P, Chi YR. Carbene-catalyzed and pnictogen bond-assisted access to P^{III}-stereogenic compounds. *Angew Chem Int Ed Engl*. 2024;63(28):Article e202404477.
87. Li X, Duan M, Deng Z, Shao Q, Chen M, Zhu G, Houk KN, Sun J. Catalytic enantioselective synthesis of chiral tetraarylmethanes. *Nat Catal*. 2020;3:1010–1019.
88. Dai L, Liu Y, Xu Q, Wang M, Zhu Q, Yu P, Zhong G, Zeng X. A dynamic kinetic resolution approach to axially chiral diaryl ethers by catalytic atroposelective transfer hydrogenation. *Angew Chem Int Ed Engl*. 2023;62(7):Article e202216534.
89. Bao H, Chen Y, Yang X. Catalytic asymmetric synthesis of axially chiral diaryl ethers through enantioselective desymmetrization. *Angew Chem Int Ed Engl*. 2023;62(14):Article e202300481.
90. Zhou B-A, Li X-N, Zhang C-L, Wang Z-X, Ye S. Enantioselective synthesis of axially chiral diaryl ethers via NHC catalyzed desymmetrization and following resolution. *Angew Chem Int Ed Engl*. 2024;63(4):Article e202314228.
91. Han X, Chen L, Yan Y, Zhao Y, Lin A, Gao S, Yao H. Atroposelective synthesis of axially chiral diaryl ethers by copper-catalyzed enantioselective alkyne–azide cycloaddition. *ACS Catal*. 2024;14(5):3475–3481.
92. Benincori T, Celentano G, Pilati T, Ponti A, Rizzo S, Sannicol F. Configurationally stable molecular propellers: First resolution of residual enantiomers. *Angew Chem Int Ed*. 2006;45:6193–6196.
93. Mislow K. Stereochemical consequences of correlated rotation in molecular propellers. *Acc Chem Res*. 1976;9(1):26–33.
94. Lorkowski J, Bouetard D, Yorkgitis P, Gembicky M, Roisnel T, Vanthuyne N, Munz D, Favereau L, Bertrand G, Mauduit M, et al. Circularly polarized luminescence from cyclic (alkyl) (amino) carbene derived propellers. *Angew Chem Int Ed Engl*. 2023;62(33):Article e202305404.